Table 1 Comparison of results (Mach 20, 20 km)

	Normalized distance from wall r_n[a]					
	0.0		0.50		1.0	
	Present	Ref. 18	Present	Ref. 18	Present	Ref. 18
$\frac{p}{p_\infty}$	533.4	536.9	527.4	532.3	506.6	511.7
$\frac{\rho}{\rho_\infty}$	11.91	11.85	11.86	11.76	11.40	11.37
$T(K)$	7283	7395	7252	7388	7243	7357
Mole fraction						
O	0.2951	0.2933	0.2957	0.2928	0.2958	0.2933
O_2	1.089-3	9.265-4	1.123-3	9.232-4	1.091-3	9.232-4
N	0.1967	0.2003	0.1915	0.1996	0.1931	0.1970
N_2	0.4851	0.4776	0.4894	0.4780	0.4881	0.4801
NO	2.133-2	2.070-2	2.143-2	2.065-2	2.106-2	2.057-2
e^-	3.927-4	3.945-4	3.821-4	3.921-4	3.828-4	3.840-4

[a] $r_n = 0$ at the wall; $r_n = 1$ at the shock.

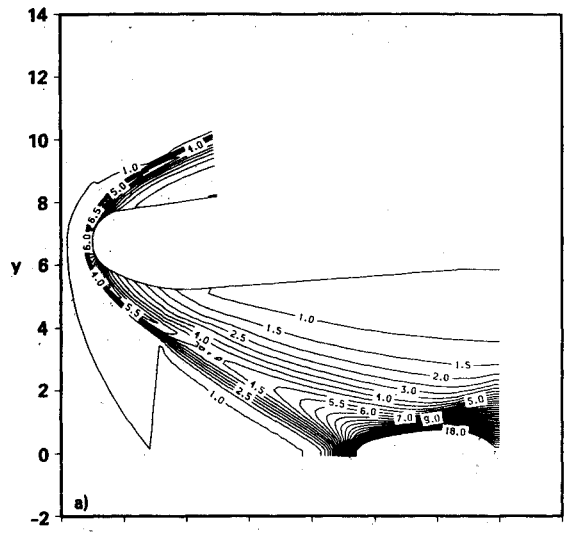

a) Normalized density

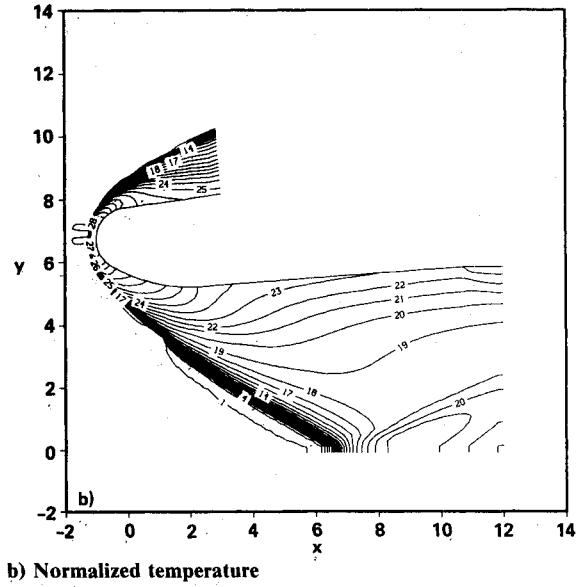

b) Normalized temperature

Fig. 4 Hypersonic inlet, Mach 20.

The temperature along much of the forebody surface is in excess of 7000 K. Figure 4 shows equilibrium flow through a hypersonic inlet at the same conditions. This problem was chosen to demonstrate the code's ability to compute internal as well as external flows. Only the upper half of the axisymmetric inlet is shown. Some interesting flow phenomenon is apparent, including a Mach stem and a reflected shock. No significant problems were encountered when the code was applied to these more complex configurations.

Conclusions

The objective of this work was to develop an algorithm that could accurately predict inviscid, equilibrium, high Mach number flows. That goal has been achieved. The method has proved its ability to capture strong shocks. Solutions for a generic axisymmetric hemisphere at Mach 20 compare well with previously published results. The code has shown its ability to be applied to both internal and external hypersonic flows over a variety on configurations.

References

[1]Gnoffo, P. A., "Application of Program LAURA to Three Dimensional AOTV Flowfields," AIAA Paper 86-0565, Jan. 1986.

[2]Balakrishnan, A., Davy, W. C., and Lombard, C. K., "Real-Gas Flowfields about Three Dimensional Configurations," *Journal of Spacecraft and Rockets,* Vol. 22, Jan.-Feb. 1985, pp. 46-53.

[3]Eberhardt, S. and Palmer, G. E., "A Two Dimensional TVD Scheme for Inviscid, High Mach Number Flows in Chemical Equilibrium," AIAA Paper 86-1284, 1986.

[4]Steger, J. L. and Warming, R. F., "Flux Vector Splitting of the Inviscid Gasdynamic Equations with Application to Finite Difference Methods," NASA TM-78605, 1979.

[5]Gordon, S. and McBride, B. J., "Computer Program for Calculation of Complex Chemical Equilibrium Compositions, Rocket Performance, Incident and Reflected Shocks, and Chapman-Jouquet Detonations," NASA SP-273, 1976.

[6]Steger, J. L., "Implicit Finite-Difference Simulation of Flow about Arbitrary Two Dimensional Geometries," *AIAA Journal,* Vol. 16, July 1978, pp. 679-686.

[7]Beam, R. M. and Warming, R. F., "An Implicit Factored Scheme for the Compressible Navier-Stokes Equations," *AIAA Journal,* Vol. 16, April 1978, pp. 393-402.

[8]Stull, D. R. and Prophet, H., *JANAF Thermochemical Tables,* 2nd ed., National Standard Reference Data System NBS37, June 1971.

[9]Nakahashi, K. and Deiwert, G. S., "A Self-Adaptive-Grid Method with Application to Airfoil Flow," AIAA Paper 85-1525, July 1985.

[10]Lyubimov, A. N. and Rusanov, V. V., "Gas Flows Past Blunt Bodies, Part II: Tables of the Gas-Dynamic Functions," NASA TT-F715, 1973.

Deforming Grid Method Applied to the Inverse Problem of Heat Conduction

R. C. Mehta* and T. Jayachandran†
Vikram Sarabhai Space Centre, Trivandrum, India

Nomenclature

c = heat capacity of the material
h = heat-transfer coefficient
k = thermal conductivity
L = thickness of material

Received Dec. 24, 1986; revision received Sept. 30, 1987.

*Engineer, Aerodynamics Division.
†Engineer, Solid Motor Project.

q_w = surface heat flux
T = nodal temperature
T_{aw} = adiabatic wall temperature
T_0 = initial condition for temperature
t = time variable
X = Cartesian coordinate with respect to fixed reference
α = thermal diffusivity
Δt = computing time interval
δ = heat penetration depth
ρ = material density
ϕ_j = finite-element shape functions

Introduction

IN the inverse heat-conduction problem,[1] the prediction of transient wall heat flux is accomplished by inverting the temperature history as measured by a thermocouple located at the inner or outer surface of the solid material. The finite-difference and finite-element methods[2,3] have been the predominant numerical techniques for the solution of the inverse heat-conduction problem. A potential difficulty with numerical techniques in the solution of the inverse heat-conduction problem is the lack of a priori information concerning the gradient in the dependent variable to be estimated. Therefore, a predetermined distribution of nodal points is either inadequate or computationally uneconomical. What is needed is a method wherein the distribution of nodal points is to be adjusted in response to the nature of the computed solution.

Lynch and O'Neill[4] have used continuously deforming finite elements in space and a finite-difference scheme for the integration in time to solve the Stefan problem. This method has great intuitive appeal, provides a rationale and a mechanism for generating difference equations on a nonuniform grid, and also allows the use of higher elements in regions where they are suited to the physics of the problem. In the absence of grid deformation, the method reduces exactly to the conventional Galerkin finite-element procedure.[5] The particular method of solution in time may still be specified by the user to suit the detail of the specific problem; it is not dictated by the moving mesh feature.

The purpose of the present Note is to analyze an inverse heat-conduction problem using a finite-element and deforming grid technique in conjunction with measured thermocouple temperature at the outer surface of the finite slab. An explicit deformation pattern via a heat penetration depth concept[6] is employed for adequate modeling of the transient steep gradient and the time delay in temperature response resulting from the surface and thermocouple location. The proposed scheme is shown to be accurate, efficient, and convenient.

Analysis

Consider the one-dimensional heat-conduction equation with constant thermophysical properties of material. The physical problem is that of a slab of finite thickness exposed to a transient heat input at one surface and perfect insulation at the other. For the system under consideration, the governing heat-conduction equation is

$$k\frac{\partial^2 T}{\partial X^2} = \rho c\frac{\partial T}{\partial t}, \qquad 0 < X < 1 \tag{1}$$

with the boundary conditions

$$-k\frac{\partial T(0,t)}{\partial X} = q_w, \qquad t > 0 \tag{2}$$

$$\frac{\partial T(L,t)}{\partial X} = 0, \qquad t > 0 \tag{3}$$

and the initial condition

$$T(X,0) = T_0 \qquad \text{for all } X \tag{4}$$

Deforming Finite-Element Formulation

It is appropriate to discretize the diffusion equation in terms of deforming finite elements in order to treat the transient steep gradient of wall heat flux near the boundary of the heated surface. The spatial shape functions ϕ_j in the Galerkin weak form of the equations will be time-dependent at every fixed location X_j and can be written as

$$T(X,t) = T_j(t)\phi_j(X,t), \qquad j = 1,2,3,\ldots,N \tag{5}$$

where the T_j are the N nodal values of the temperature acting as generalized coordinates of the problem. The time derivative of the temperature is accordingly discretized as

$$\frac{\partial T}{\partial t} = \phi_j\frac{\mathrm{d}T_j}{\mathrm{d}t} + T_j\frac{\partial \phi_j}{\partial t} \tag{6}$$

and implies, contrary to conventional fixed-grid formulation, the time rate of change of the shape function. Using the isoparametric element and the Langrangian nature of the finite-element approximation, the term $\partial\phi_j/\partial t$ is evaluated as[7]

$$\frac{\partial \phi_j}{\partial t} = -\frac{\mathrm{d}X}{\mathrm{d}t}\cdot\nabla\phi_j \tag{7}$$

The term $\mathrm{d}X/\mathrm{d}t$ is the mesh deformation velocity and is continuous throughout the spatial domain. Assembling Eqs. (6) and (7) yields

$$\frac{\partial T}{\partial t} = \phi_j\frac{\mathrm{d}T_j}{\mathrm{d}t} - \frac{\mathrm{d}X}{\mathrm{d}T}\cdot\nabla T \tag{8}$$

The last term in the Eq. (8) can be viewed as a transport term accordingly for the convective effect of mesh motion.

Following the usual Galerkin procedure, one obtains the heat-conduction equation in the form of a system of semidiscretized differential equations in terms of nodal temperature, collected in the global vector $\bar{T}$ as

$$(\bar{K} - \bar{K}^d)\bar{T} + \bar{C}\dot{\bar{T}} = \bar{g} \tag{9a}$$

where a superscript dot denotes time partial differentiation, and $\bar{K}$, $\bar{K}^d$, $\bar{C}$, and $\bar{g}$ are the conventional thermal conductivity matrix, the convective matrix accounting for mesh deformation, the heat capacitance matrix, and the thermal load vector, respectively, with typical components of the form

$$K_{ij} = k\int_0^L \frac{\partial\phi_i}{\partial X}\cdot\frac{\partial\phi_j}{\partial X}\,\mathrm{d}X$$

$$K^d_{ij} = \rho c\int_0^L \frac{\mathrm{d}X}{\mathrm{d}t}\cdot\frac{\partial\phi_j}{\partial X}\phi_i\,\mathrm{d}X$$

$$C_{ij} = \rho c\int_0^L \phi_i\phi_j\,\mathrm{d}X$$

$$g_1 = q_w, \qquad g_j = 0, \qquad j = 2,3,\ldots,N \tag{9b}$$

All of these characteristic matrices depend on time and the unknown surface heat flux q_w. Conventional heat-conduction fixed-grid formulations are simply obtained by omitting the convective matrix $\bar{K}^d$ in Eq. (9). Equation (9) is now integrated in time, using a modified Galerkin scheme[4] at time t^* as

$$t^* = t_n + \epsilon\,\Delta t \tag{10}$$

$$\left[\frac{\bar{C}}{\Delta t} + \epsilon(\bar{K} - \bar{K}^d)\right]^* \bar{T}_{n+1} = \left[\frac{\bar{C}}{\Delta t} - (1-\epsilon)(\bar{K} - \bar{K}^d)\right]^* \bar{T}_n + \bar{g} \tag{11}$$

where the subscripts denote the corresponding time station. The value of ϵ is taken as 2/3. This algorithm possesses

Table 1 Wall heat flux at various grid arrangements

		Uniform grid			Nonuniform grid			Deforming grid			
t,s	T_M at outer surface, K	T_s, K	$q_w \times 10^6$, W/m^2	h, W/m^{2}K	T_s, K	$q_w \times 10^6$, W/m^2	h, W/m^{2}K	T_s, K	$q_w \times 10^6$, W/m^2	h, W/m^{2}K	h_B, W/m^{2}K [a]
1	300	658.3	3.7155	1624.1	671.0	3.8462	1690.6	745.3	4.5173	2052.7	2254.2
2	300	763.4	3.7155	1702.3	765.2	3.8462	1763.4	877.2	4.5173	2183.5	2254.2
3	300	883.7	3.7155	1801.6	892.9	3.8462	1873.4	1051.1	4.5173	2339.5	2254.2
4	300	971.5	3.7155	1881.7	978.6	3.8462	1954.5	1111.6	4.5173	2462.5	2254.2
5	300	1053.9	3.7155	1963.9	1063.7	3.8462	2043.4	1072.9	4.5173	2411.6	2254.2
6	326	1054.6	3.7155	1964.5	1067.9	3.8462	2044.9	1074.0	4.5173	2413.1	2254.2
7	342	1028.9	2.7008	1408.8	1046.4	2.8486	1499.6	1049.5	2.8180	1485.9	2254.2
8	356	1067.5	2.6982	1436.9	1091.8	2.8399	1531.6	1081.9	2.8201	1512.8	2254.2
9	380	1097.4	2.7045	1463.0	1124.4	2.8596	1569.8	1115.4	2.8425	1552.8	2254.2
10	402	1132.5	2.7047	1491.4	1163.3	2.8583	1603.3	1152.2	2.8463	1586.7	2254.2
11	425	1165.9	2.7038	1518.9	1178.7	2.8526	1632.6	1188.1	2.8451	1618.5	2254.2
12	440	1198.9	2.6908	1539.7	1231.5	2.8054	1636.2	1221.8	2.8117	1630.8	2254.2
13	460	1231.2	2.6829	1564.6	1263.4	2.7758	1649.7	1255.1	2.7910	1650.6	2254.2
14	479	1262.9	2.6728	1588.1	1293.6	2.7383	1657.1	1286.9	2.7640	1665.9	2254.2
15	507	1238.5	2.0941	1226.4	1253.8	2.0147	1190.6	1253.0	2.0915	1235.4	2254.2
16	528	1252.9	2.0856	1231.8	1264.6	1.9815	1178.5	1266.7	2.0675	1231.6	2254.2

[a] h_B = heat-transfer coefficient (Bartz).[11]

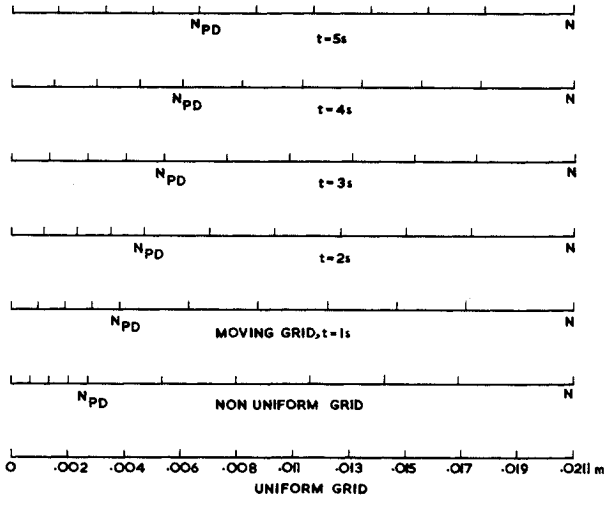

Fig. 1 Finite slab discretization.

unconditional stability and accuracy and is also free from oscillatory behavior.[8] But in Eq. (11), the surface heat flux q_w is an unknown parameter; thus, the solution of the complete problem from $X = 0$ to X_M cannot be readily obtained because the boundary condition is not known but, rather, the temperature history is known at an interior point X_M. In estimating, one minimizes

$$F(q_w,t) = |T_c(X_M,t) - T_M(X_M,t)| \tag{12}$$

where T_c and T_M are, respectively, the calculated and measured thermocouple temperature at (X_M,t). The above-mentioned minimization scheme is found suitable when a single thermocouple is used to measure the temperature history and also a larger time step in the computation is employed in order to satisfy the larger time interval of measurement. The calculated temperature is, in general, a nonlinear function of q_w. Hence, to predict the unknown surface condition, an iteration is required in this method, which is a disadvantage. A simple procedure approximates at each iteration the calculated temperature by a Newton-Raphson iteration procedure[9] (with quadratic convergence). This iteration scheme begins with an initial value of q_w and continues until, say, $|F| \le 10^{-4}$.

Deforming Grid Strategy

It is observed that the temperature response at an interior location or outer surface is delayed and damped with respect to changes at the surface of the body.[10] This leads to numerical difficulties in determining the unknown wall heat flux. It stems from boundary condition (2) that the correct estimation of the q_w will depend heavily on the ability of the deforming grid technique to represent accurately the interior gradient near the surface. In many aerospace applications, such as re-entry and rocket nozzle heat-transfer problems, the sharp fronts in the temperature distribution are found near the heated surface; therefore, such a steep thermal gradient must be dealt with using the deforming grid technique. A fine mesh in the vicinity of the boundary within the zone of a heat penetration depth[6] allows for a suitable and accurate solution to this problem. This analysis included N_{PD} elements of the initial (uniform or nonuniform) grid in a zone $\delta(t) = (\alpha t)^{\frac{1}{2}}$ corresponding to the instantaneous heat penetration depth. The N_{PD} elements are dilated, and the remaining ones are contracted using the following instantaneous coordinates locations:[6]

$$X_j(t) = \frac{X_j^0}{X_m^0} X_m(t),\ j = 1,2,\ldots,m$$

$$X_j(t) = X_m(t) + [L - X_m(t)] \frac{(X_j^0 - X_m^0)}{(L - X_m^0)},\ j = m+1,\ldots,N \tag{13}$$

where $m = N_{PD}$, $X_m(t) = \delta(t)$ and X_j^0 are the initial node positions with respect to fixed origin. The deforming grid strategy is carried out in the preceding formulation as long as no temperature rise from the initial temperature is observed by the thermocouple. Once this delay in the measurement of temperature history is over, the deforming grid strategy is stopped and the solution continues with that grid. The heat penetration depth is an explicit function of time.

Example

Moving-grid finite-element formulation, discussed in the previous sections, has been utilized for estimation of the wall heat flux and the surface temperature at the inner surface for a typical divergent rocket nozzle made of mild steel in conjunction with the experimentally measured outer surface temperature data in a static test. The nozzle conditions and material properties taken are: $L = 0.0211$ m, $T_0 = 300$ K, $T_{aw} = 2946$ K, thermal conductivity (average) = 35 W/m^{2}K, $\rho = 7900$ kg/m^3, $c = 545$ Ws/kg · K, burning time = 16 s. The heat input consists of a convective heat flux at the inner surface ($X = 0$). The $X = L$ is insulated. An insulated chromel/alumel thermocouple of 30 gage was used for measuring the temperature history at the outer surface. A time delay of 6 s was noticed in the measurement of temperature history.

In the determination of wall heat flux, three different types of grid arrangements (namely, uniform, nonuniform, and deforming grids) were used in conjunction with the above-mentioned Newton-Raphson iteration procedure. An iterative index is included in the computer program to count the number of iterations necessary to achieve desired accuracy in the minimization of the function $|F|$. In each case, 11 nodes and a time interval of 1 s are taken for computational purposes. In the case of nonuniform grid, 5 meshes are stretched near the convectively heated surface of the slab while the remaining mesh covers the rest of the region. Figure 1 shows the mesh movement at each time interval using the heat penetration depth concept. The numerical computations have been performed on a CDC 170/730 digital computer. The convective heat-transfer coefficient can be calculated as

$$h = q_w/(T_{aw} - T_s) \tag{14}$$

where T_s is the surface temperature. Table 1 depicts predicted values of wall heat flux, surface temperature, and convective heat-transfer coefficient using the three different kinds of grid arrangements. It can be seen from the table that for $t \leq 6$ s, the heat-transfer coefficient obtained using the deforming grid strategy is in good agreement with the calculated results of Bartz.[11] Thus, the current numerical analysis shows that the moving-grid finite-element formulation gives an adequate modeling of the transient steep gradient of wall heat flux near the boundary of the heated surface. But for $t > 6$ s, fixed and deforming grid results tend to coincide since spatial grids become identical, as shown in Fig. 1. The estimated values of heat-transfer coefficient calculated using three different type of grid arrangements are somewhat lower than the calculated results of Bartz for $t > 6$ s. The predicted value of the heat-transfer coefficient shows that the Bartz equation gives a conservative estimation of the heat-transfer coefficient. This is also demonstrated in the previous analysis.[12] The maximum number of iterations per step are 11 and 8 for the uniform and nonuniform grids, respectively, whereas it is reduced to 4 iterations per step in the case of deforming grid. This example thus reveals that the deforming grid is economical in terms of CPU time compared to the other type of grid arrangements. This example also demonstrates that the arbitrary mesh deformation can be conveniently accommodated in the solution to the inverse problem of heat conduction. It is also important to mention here that geometrical conservation is maintained using nonuniform and deforming grids in the analysis because the numerical computations are carried out in the physical plane.

Conclusions

A mesh coupling thermal conductivity matrix with deforming finite-element formulation with heat penetration depth concept is found useful to treat the initial time delay in temperature response. The deforming grid procedure has shown itself to reduce substantially the number of iterations per step to achieve the required tolerance in the analysis of the inverse heat-conduction problem.

References

[1]Beck, J. V., Blackwell, B., and St. Clair, C. R. Jr., *Inverse Heat Conduction Problem*, Wiley, New York, 1985.

[2]Mehta, R. C., "An Efficient Numerical Method for Solving Inverse Heat Conduction Problem in a Hollow Cylinder," *AIAA Journal*, Vol. 22, June 1984, pp. 860–862.

[3]Bass, B. R., "Application of the Finite Element Method to the Nonlinear Inverse Heat Conduction Problem Using Beck's Second Method," *Journal of Engineering for Industry*, Vol. 102, May 1980, pp. 168–176.

[4]Lynch, D. R. and O'Neill, K. "Continuously Deforming Finite Elements for the Solution of Parabolic Problems, With and Without Phase Change," *International Journal for Numerical Methods in Engineering*, Vol. 17, 1981, pp. 81–96.

[5]Zienkiewicz, O. C., *The Finite Element Method in Engineering Science*, McGraw-Hill, London, 1971.

[6]Hogge, M. and Gerrekens, P., "Steep Gradient Modeling in Diffusion Problems", *Numerical Method in Heat Transfer II*, edited by R. W. Lewis, K. Morgan, and B. A. Schrefler, Wiley, New York, 1983, pp. 73–93.

[7]Lynch, D. R. and Gray, W. G., "Finite Element Simulation of Flow in Deforming Regions," *Journal of Computational Phyics*, Vol. 36, July 1980, pp. 135–153.

[8]Owen, D. R. J. and Damjanic, F., "The Stability of Numerical Time Integration Techniques for Transient Thermal Problems with Special Reference to Integration Effects," *Numerical Methods in Thermal Problems, Proceedings of the 2nd International Conference*, edited by R. W. Lewis, K. Morgan, and B. A. Schreffer, Pineridge Press, 1981, pp. 487–505.

[9]Mehta, R. C., "Numerical Solution of Nonlinear Inverse Heat Conduction Problem with a Radiation Boundary Condition," *International Journal for Numerical Methods in Engineering*, Vol. 20, 1984, pp. 1057–1066.

[10]Beck, J. V., "Nonlinear Estimation Applied to the Nonlinear Inverse Heat Conduction Problem," *International Journal of Heat and Mass Transfer*, Vol. 13, April 1970, pp. 703–716.

[11]Bartz, D. R., "A Simple Equation for Rapid Estimation of Rocket Nozzle Convective Heat Transfer Coefficients," *Jet Propulsion*, Vol. 27, Jan. 1957, pp. 49–51.

[12]Mehta, R. C., "Solution of the Inverse Conduction Problem," *AIAA Journal*, Vol. 15, Sept. 1977, pp. 1355–1356.

Approximate Method for Transient Conduction in Arbitrarily Shaped Solids with a Volumetric Heat Source

K. Taghavi* and R. A. Altenkirch†
University of Kentucky, Lexington, Kentucky

Introduction

THE lumped-heat-capacity technique has long been used to predict transient thermal behavior of solids when the Biot number is small compared to unity.[1] A small Biot number implies a negligible spatial temperature variation within the solid. This method, when applicable, is simple and powerful because it may be applied to any geometry.

In this work, a quasi-steady-state model is considered for solids with internal heat generation and arbitrary Biot number. It is assumed that the temperature profile in the solid at any instant in time is similar to that of the steady state. The basis of this approach has been explained by Arpaci[2] and parallels that for thermally fully developed internal flows. A fully developed regime has been identified for unsteady conduction in solids with convective boundary conditions, but without heat generation.[3] Here, we consider the presence of a heat source, the steady state becomes analogous to fully developed internal flow, and the temporal behavior of the temperature field is contained in the behavior of the mass-averaged (bulk) temperature. The approach will be shown to be more accurate than the lumped-heat-capacity technique and is easily applied to solids with arbitrary shapes.

Received April 10, 1987; revision received Jan. 29, 1988.

*Assistant Professor, Department of Mechanical Engineering.

†Professor, Department of Mechanical Engineering; currently at Department of Mechanical and Nuclear Engineering, Mississipi State University.